

## LATTICE THERMAL CONDUCTIVITY IN A HOLLOW SILICON NANOWIRE

WEI-QING HUANG<sup>†</sup>, KE-QIU CHEN<sup>\*,†,‡</sup>, Z. SHUAI<sup>‡,§</sup>,  
LINGLING WANG<sup>†</sup> and WANGYU HU<sup>†</sup>

<sup>†</sup>*Department of Applied Physics, Hunan University, Changsha 410082, China*

<sup>‡</sup>*Laboratory of Organic Solids, Center for Molecular Sciences,  
Institute of Chemistry, Chinese Academy of Sciences, 100080 Beijing, China*

<sup>\*</sup>*keqichen@iccas.ac.cn*

<sup>§</sup>*zqshuai@iccas.ac.cn*

Received 27 December 2004

We theoretically investigate the lattice thermal conductivity of a hollow Si nanowire under the relaxation time approximation. The results show that the thermal conductivity in such structure is decreased markedly below the bulk value due to phonon confinement and boundary scattering. The thermal conductivities under different scattering mechanisms are given, and it is found that the boundary scattering is dominant resistive process for the decrease of the thermal conductivity.

*Keywords:* Heat conduction; phonons; nanoscale materials.

PACS numbers: 44.10.+i, 63.22.+m, 61.46.+w

### 1. Introduction

One-dimensional nanostructures such as nanowires and nanotubes are anticipated to play a key role in the miniaturization of microelectronic devices and circuits as well as to provide model systems to demonstrate quantum size effects.<sup>1,2</sup> Thermal conductance of these structures are attracting increasing attention due to its importance in controlling the performance and stability of nanometer devices.<sup>3</sup> At low enough temperatures, the ballistic quantized thermal transport due to the discrete mode structure of the thermal pathway has been studied experimentally<sup>4</sup> and theoretically.<sup>5–10</sup> As far as diffusive thermal conductance is concerned, many theoretical investigations have reported the thermal conductivity of semiconductor nanowires, including Si,<sup>11–15</sup> CdTe,<sup>16</sup> and GaAs wires.<sup>17,18</sup> These studies predicted that the thermal conductivity of semiconductor nanowires are more about an order or two orders of magnitude smaller than those of bulk crystals. Recently, experimental<sup>19</sup> and theoretical<sup>20,21</sup> studies show that the thermal conductivity of Si nanowires with diameters of 22–115 nm was more than two orders of magnitude lower than their bulk value. These works indicate that the thermal conductivity

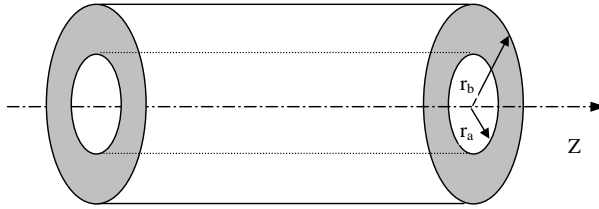


Fig. 1. Structure of a hollow Si cylindrical nanowire.  $r_a$  and  $r_b$  are inner and outer radii, respectively.  $z$  is taken along the axial direction of the nanowire.

depends strongly on the geometry and diameter of the nanowires. In order to study the effect contributed from the geometric configuration, Zeng *et al.*<sup>22</sup> studied temperature distribution and equivalent thermal conductivity for nano- and micro-thin films with cylindrical and spherical geometries, and found a significant drop in temperature occurring at interfaces. Using the lattice Boltzmann (LB) method, Jiaung *et al.*<sup>23</sup> analytically investigated the phonon heat conduction in a free standing, straight and bent nanoduct. They found that the size effect depends dramatically on the phonon Knudsen number.

Motivated by these works, the present paper investigates the phonon heat transport along the axial direction in a hollow silicon nanowire, schematically shown in Fig. 1. The hollow Si nanowire may be a suitable model to simulate a silicon nanotube. Although there is still no report about the silicon nanotube being synthesized experimentally, several theoretical studies have been done to explore the existence and the properties of silicon nanotubes.<sup>24–27</sup> It is predicted that silicon nanotube can in principle be synthesized. Our results show that the thermal conductivity decreases with the increase of the inner radius when the outer radius of the hollow nanowire is fixed. The boundary scattering is dominant resistive process for the reduction of the thermal conductivity in such a hollow nanowire, and it is more sensitive to the variation of the inner radius than other scattering such as Umklapp scattering, mass-difference scattering, or phonon-electron scattering.

This paper is organized as follows: Sec. 2 gives a brief description of the model and the formulae used in calculations. The calculated results are presented in Sec. 3 with analysis. Finally, a summary is given in Sec. 4.

## 2. Model and Formalism

A hollow silicon nanowire with inner radius  $r_a$  and outer radius  $r_b$  is considered in Fig. 1. Using the relaxation-time methods by following Klemen's and Callaway's derivation, we can obtain the regular bulk formula for the lattice thermal conductivity as<sup>28,29</sup>

$$\kappa_{ph} = \frac{k_B}{2\pi^2V} \left( \frac{k_B T}{\hbar} \right)^3 \int_0^{\theta_D/T} \frac{\tau_c x^4 e^x}{(e^x - 1)^2} dx \quad (1)$$

where  $x = \hbar\omega/k_B T$ ,  $k_B$  is the Boltzmann constant,  $\hbar$  the Plank constant,  $\theta_D$  the Debye temperature,  $\tau_c$  the combined relaxation time, and  $V$  the phonon group velocity.

For simplicity we assume that the material of the hollow nanowire considered here has an isotropic symmetry and it is independent on the azimuth, and that the contribution to heat transfer along the axis of the hollow nanowire is mainly attributed to the longitudinal acoustic phonons modes as a qualitative analysis. Following the method given by Gazis,<sup>30</sup> the phonon dispersion relations can be obtained. Numerical calculated results show that different branches have different group velocities. In order to determine the resultant group velocity, we have to find the functional dependence of the phonon group velocity on phonon energy. We weight the average group velocity as a function of phonon energy as follows:

$$\bar{V}(\hbar\omega) \cong \frac{\sum_n V_n(\hbar\omega) N_n(\hbar\omega)}{\sum_n N_n(\hbar\omega)} \tag{2}$$

where  $V_n = d\omega_n/dq$  is phonon group velocity for the  $n$ th branch, and  $\omega_n$  the phonon frequency for the  $n$ th branch.  $N_n(\hbar\omega)$  is the number of oscillators with frequency  $\omega$  on the  $n$ th mode.  $N_n$  is defined by the equilibrium occupancy which is given by the Bose–Einstein distribution

$$N_n = \frac{1}{\exp\left(\frac{\hbar\omega_n}{k_B T}\right) - 1} . \tag{3}$$

However, rigorous calculation of the overall average phonon group velocity of the all contributing modes is very difficult. Equation (2) is only an approximation since the energy spacing for different phonon modes is nonequidistant. In the present paper, we only take into account the average phonon group velocity coming from the finite modes, which is enough to be used for the qualitative evaluation of the lattice thermal conductivity.

In our model, we consider acoustic phonon relaxation in resistive processes, such as phonon anharmonic interactions (three-phonon Umklapp process), mass difference (impurities) scattering, phonon-electron scattering, and boundary scattering. The combined phonon relaxation time  $\tau_c$  can be obtained from the Matthiessen’s rule

$$\tau_c^{-1} = \tau_U^{-1} + \tau_M^{-1} + \tau_{ph-e}^{-1} + \tau_B^{-1} \tag{4}$$

where  $\tau_U^{-1}$ ,  $\tau_M^{-1}$ ,  $\tau_{ph-e}^{-1}$ , and  $\tau_B^{-1}$  are the phonon relaxation rates of the three-phonon Umklapp, mass difference (impurities), phonon-electron, and boundary scattering, respectively.

By modifying the expression for  $\tau_U$  given by Slack<sup>31</sup> via introduction of the modification of group velocity due to the spatial confinement the Umklapp scattering

rate can be calculated from

$$\frac{1}{\tau_U} = \alpha \frac{\hbar\gamma^2\omega^2 T}{M_0 \bar{V}^2 \theta_D} \exp\left(-\frac{\theta_D}{\beta T}\right) \tag{5}$$

where  $\gamma$  is the Grüneisen anharmonicity parameter,  $\bar{V}$  is the average phonon group velocity, and  $M_0$  is the average mass of a single atom in the nanowire. There are two adjustable constants,  $\alpha$  and  $\beta$ , which can be adjusted to reproduce the value of the corresponding bulk material with the formula:<sup>32</sup>  $\tau_U^{-1} = 2\gamma^2 k_B T \omega^2 / (\mu V_0 \omega_D)$ , where  $\omega_D$  is the Debye frequency,  $V_0$  is the volume per atom, and the shear modulus  $\mu$ , which can be estimated from the formula  $\mu = v_d^2 \rho$ , where  $v_d$  is transverse acoustic speed and  $\rho$  is the mass density. The curves calculated by two formulae can be fitted quite well in the range  $300 \leq T \leq 800\text{K}$  with  $\alpha = 5.125$  and  $\beta = 68.02$ , which are used in the following calculation.

Mass-difference scattering arises due to the presence of atoms with a mass different from the average atomic mass. From the second-order perturbation theory the phonon relaxation rate on point defects is calculated using the following expression:<sup>16</sup>

$$\frac{1}{\tau_M} = \frac{V_0 \omega^4}{4\pi \bar{V}^3} \Gamma = \frac{V_0 \omega^4}{4\pi \bar{V}^3} \sum_i f_i \left(1 - \frac{M_i}{\bar{M}}\right)^2 \tag{6}$$

Here  $f_i$  is the relative concentration of the  $i$ th type atoms of mass  $M_i$ ,  $\bar{M} = \sum_i f_i M_i$  is the average atomic mass, and  $\Gamma$  is the measure of the strength of the mass-difference scattering. It is worthwhile to note that the effect of the particular geometry and boundary conditions are considered in Eq. (6) through the modification of the phonon group velocity.

In our calculation, we consider silicon with a relatively low carrier concentration of  $10^{18} \text{ cm}^{-3}$ . At such a low doping level, the relaxation time for acoustic phonons scattered by electrons can be written as<sup>33</sup>

$$\frac{1}{\tau_{ph-e}} = \frac{n_e \epsilon_1^2 \omega}{\rho \bar{V}^2 k_B T} \left(\frac{\pi m^* \bar{V}^2}{2k_B T}\right)^{1/2} \exp\left(-\frac{m^* \bar{V}^2}{2k_B T}\right) \tag{7}$$

where  $n_e$  is the concentration of conduction electrons,  $\epsilon_1$  is the deformation potential,  $\rho$  is the mass density, and  $m^*$  is the electron effective mass.

The boundary scattering in a solid nanowire<sup>12,14,16</sup> is usually treated in the Casimir limit in that all phonons that have a positive normal velocity lose the sense of their directionality and obey the equilibrium distribution when they reach the boundary. In the Casimir limit, the effective phonon mean free path is given by  $\bar{\lambda} = D$  and  $1.12L$  for a circular cylindrical quantum wire of diameter  $D$  and a rectangular quantum wire with a square cross-section with side  $L$  in the case of purely diffuse scattering, respectively.<sup>34</sup> For a hollow nanowire, there appears a new inner boundary with radius  $r_a$  other than outer boundary. So, phonon can be scattered not only by the outer wall but also by the inner wall. Based on the Casimir limit, we suppose that  $\tau$ , the relaxation time for any other processes except

boundary scattering, is so long that the phonon will make many trips back and forth between the walls before it is likely to be scattered internally. Thus, the possible maximum free path of a phonon is  $\lambda_{\max} = 2\sqrt{r_b^2 - r_a^2}$  for a hollow nanowire with fixed inner radius  $r_a$  and outer radius  $r_b$ . Since the scattering probability of the phonon is increased with the increase of the inner radius  $r_a$ , and reaches unity when  $r_a = r_b$ , we can assume that the probability of boundary scattering is proportional to  $(r_a/r_b)^p$ , which  $p(> 0)$  acts as a adjusted parameter. The effect of  $p$  on thermal conductivity is discussed numerically in Sec. 3. Therefore, as a qualitative model, it is reasonable to take the effective boundary mean free path as  $\bar{\lambda} = 2\sqrt{r_b^2 - r_a^2}[1 - (r_a/r_b)^p]$ . Then, the boundary relaxation rate in a hollow nanowire can be expressed as

$$\frac{1}{\tau_B} = \frac{\bar{V}}{2\sqrt{r_b^2 - r_a^2}[1 - (r_a/r_b)^p]}. \quad (8)$$

It is obviously seen from Eq. (8) that in the limit of  $r_a = 0$ , the relaxation rate by boundary scattering is recovered to Casimir formula of a solid nanowire, i.e.,  $\tau_B^{-1} = \bar{V}/2r_b$ .

### 3. Numerical Results and Discussion

Firstly, solving numerically the elasticity equation, we can obtain confined phonon dispersions for a hollow cylindrical Si nanowire. Hereafter, we fix the outer radius  $r_b = 20$  nm. The material parameters used in the calculation are summarized in Table 1. Then the group velocities can be obtained by numerical differentiation. Figure 2 shows the average phonon group velocity as a function of the phonon energy. It is obvious that the average phonon velocity has an oscillation for a small value of the phonon energy. With the increase of the phonon energy, the oscillation becomes smaller and gradually approaches a constant value  $5.07 \times 10^3$  m/s for

Table 1. The material parameters of silicon used in calculation.

Parameter	Value	Reference
Lattice constant $a$ (nm)	0.543	Ref. *
Crystal density $\rho$ ( $g \cdot \text{cm}^{-3}$ )	2.33	Ref. *
Atomic mass $M$ (kg)	$46.6 \times 10^{-27}$	Ref. 11
Grüneisen's constant $\gamma$	0.56	Ref. 11
Velocity of the longitudinal acoustic wave $v_l$ (cm/s)	$8.47 \times 10^5$	Ref. 14
Velocity of the transverse acoustic wave $v_t$ (cm/s)	$5.34 \times 10^5$	Ref. 14
Debye temperature $\theta_D$ (K)	625	Ref. 11
Mass-difference scattering parameter $\Gamma$	$8.357 \times 10^{-4}$	Ref. 14
Deformation potential $\varepsilon_1$ (eV)	9.5	Ref. 14
Electron effective mass $m^*$ ( $m_0$ )	0.26	Ref. 14

Ref. \*: In *Semiconductors-Basic Data*, ed. Otfried Madelung, 2., rev. ed. (Springer, Berlin, 1996), p. 15.

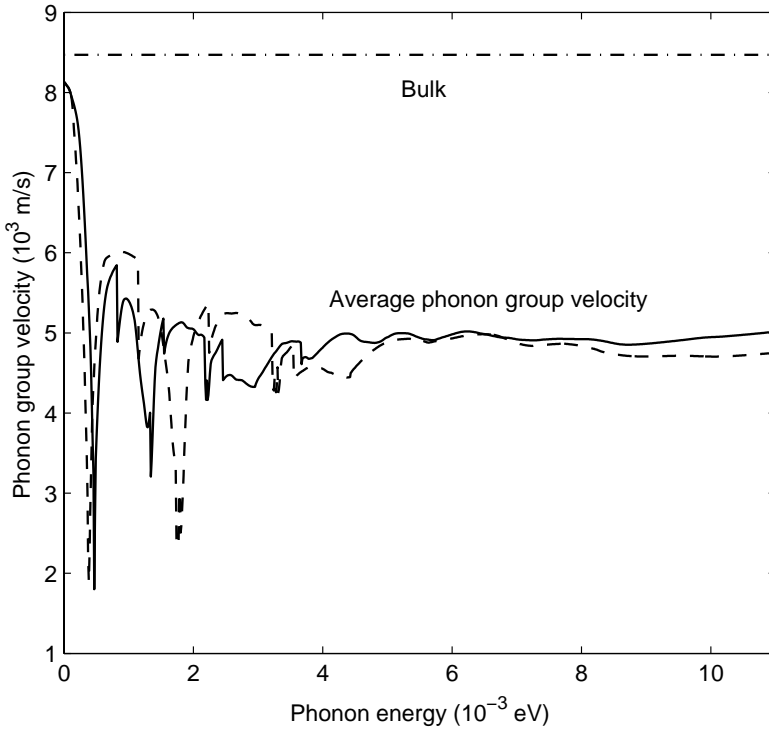


Fig. 2. Average group velocity as a function of phonon energy. Solid and dashed lines are for  $r_a = 5$  nm and 10 nm, respectively. Here we take  $r_b = 20$  nm.

$r_a = 5$  nm and  $4.75 \times 10^3$  m/s for  $r_a = 10$  nm. The overall value of the average phonon group velocities are about  $4.97 \times 10^3$  m/s and  $4.90 \times 10^3$  m/s for  $r_a = 5$  nm and 10 nm, respectively, while  $5.13 \times 10^3$  m/s for a solid nanowire with diameter  $D = 40$  nm. These results indicate that the average phonon group velocity decreases with the inner radius  $r_a$  for a fixed outer radius.

We now calculate phonon relaxation rates using Eqs. (5)–(8) for a solid nanowire, and hollow nanowires with inner radius  $r_a = 5$  nm and 10 nm, respectively. The relaxation rates for different scattering mechanisms at 300 K are shown in Fig. 3 as a function of phonon frequency. It is well known that for bulk material the Umklapp scattering dominates over others for the whole frequency range. However, it is clearly seen from Fig. 3 that the dominant scattering mechanism in the hollow nanowires is the boundary scattering when the phonons lie in the range of low frequencies frequency. Similar conclusions were obtained in the cylindrical<sup>12,14</sup> and rectangular<sup>16</sup> nanowires. Comparing Fig. 3(a) with Figs. 3(b) and 3(c), it is found that the boundary relaxation rate increases with the increasing of the inner radius  $r_a$ . This is contributed to the reduction of the mean free path of the phonon with increasing  $r_a$ . However, the relaxation rates for the three-phonon Umklapp and mass-difference scattering increase with the increasing of  $r_a$ , especially at high

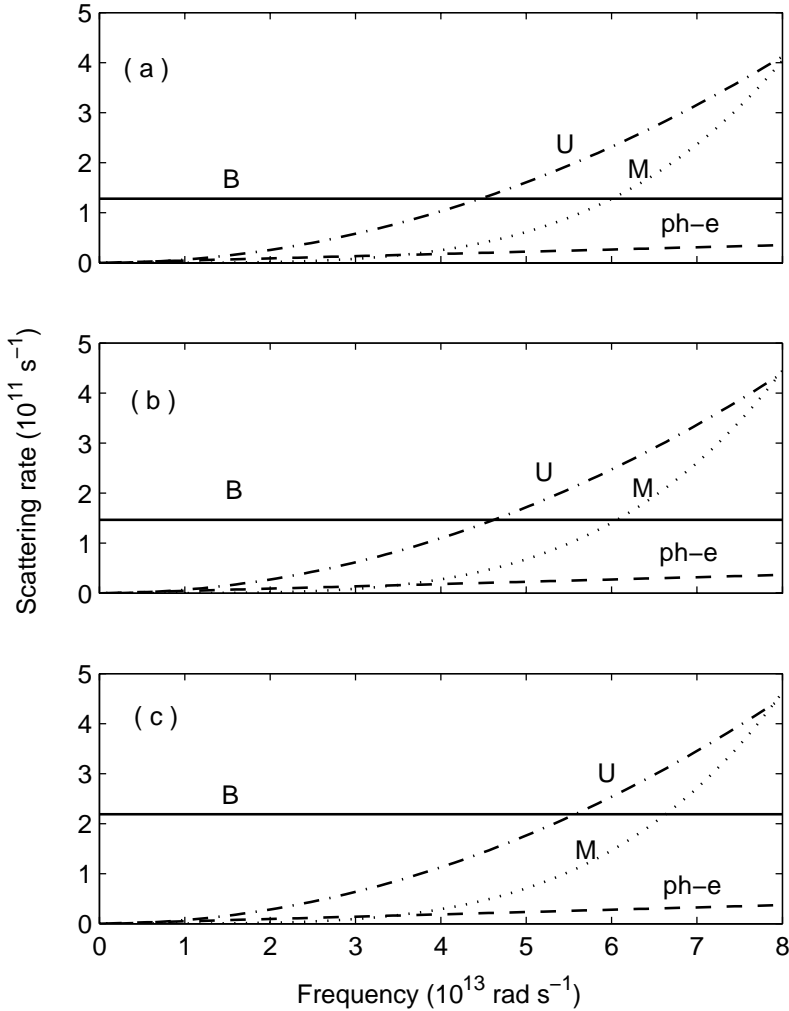


Fig. 3. Phonon scattering rates due to different scattering mechanisms as function of the phonon frequency. (a) corresponds to a solid Si nanowire with diameter  $D = 40 \text{ nm}$ , while (b) and (c) correspond to the hollow Si nanowire with inner radius  $r_a = 5 \text{ nm}$  and  $10 \text{ nm}$ , respectively. The outer radius of the hollow nanowire is  $20 \text{ nm}$ . The results are shown for three-phonon Umklapp ( $U$ ), mass-difference ( $M$ ), phonon-electron ( $ph-e$ ), and boundary scattering at  $T = 300 \text{ K}$ . Here,  $p = 1.5$ .

frequencies, which results from the combined effect of the modification of the average phonon group velocity and phonon dispersion due to the variation of geometry. These results can be understood from Eqs. (4)–(6). The relaxation rate for phonon-electron scattering is small compared to those of the above three scatterings. Note that we here take a relatively low carrier concentration ( $10^{18} \text{ cm}^{-3}$ ) in the calculation. Thus, the effect of phonon-electron scattering on the lattice thermal conductivity is weak.

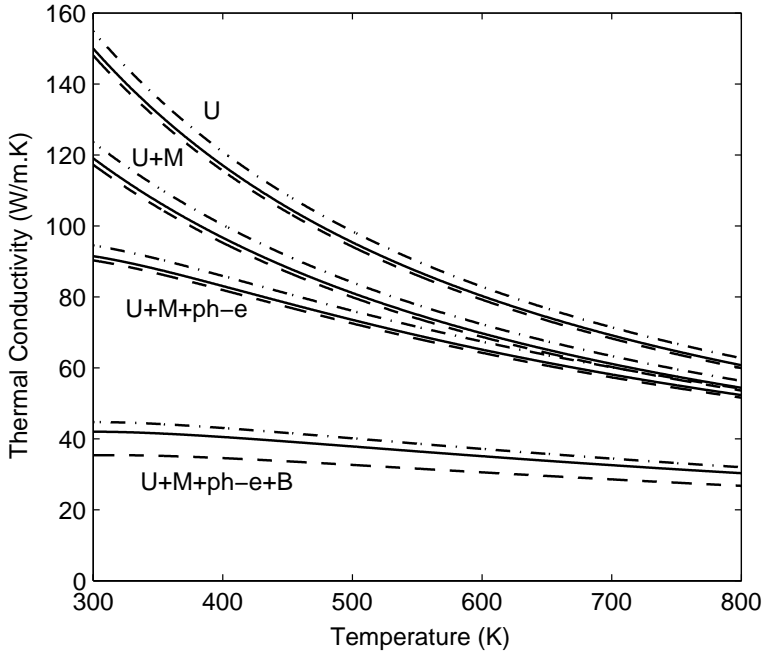


Fig. 4. Lattice thermal conductivity of hollow silicon nanowires as a function of temperature under different scattering mechanisms. The dash-dotted, solid, and dashed curves correspond to  $r_a = 0, 5,$  and  $10$  nm, respectively. Here, we fix  $p = 1.5$  and the outer radius  $r_b = 20$  nm.

Once having obtained the average phonon group velocity and the combined relaxation time, it is now straightforward to calculate the lattice thermal conductivity of the hollow silicon cylindrical nanowire for the temperature range of 300–800 K by using Eq. (1). Figure 4 shows the phonon thermal conductivity of a solid nanowire and hollow nanowires with inner radius  $r_a = 5$  nm and 10 nm as a function of temperature. As expected, the lattice thermal conductivities of the solid and hollow nanowires are much lower than the bulk silicon value in the temperature range  $T = 300 \sim 800$  K. This is mainly attributed to the reduction of the group velocity due to spatial confinement and boundary scattering, which has been demonstrated by many works.<sup>11,12,14,16,19,20</sup> To further clearly reveal the origin of the reduction in heat conductivity, we also show the lattice thermal conductivity under different scattering mechanisms in Fig. 4. When only Umklapp scattering process is considered, the thermal conductivity decreases rapidly with the increase of temperature. Moreover, the thermal conductivity is decreased slightly with the increase of the inner radius  $r_a$ . When we further consider mass difference scattering, phonon-electron scattering, and boundary scattering, the thermal conductivity continues to decrease. It is obvious from Fig. 4 that the boundary scattering leads to a dramatic decrease of the lattice thermal conductivity, and the boundary scattering is more sensitive to the variation of the inner radius  $r_a$ . This indicates that

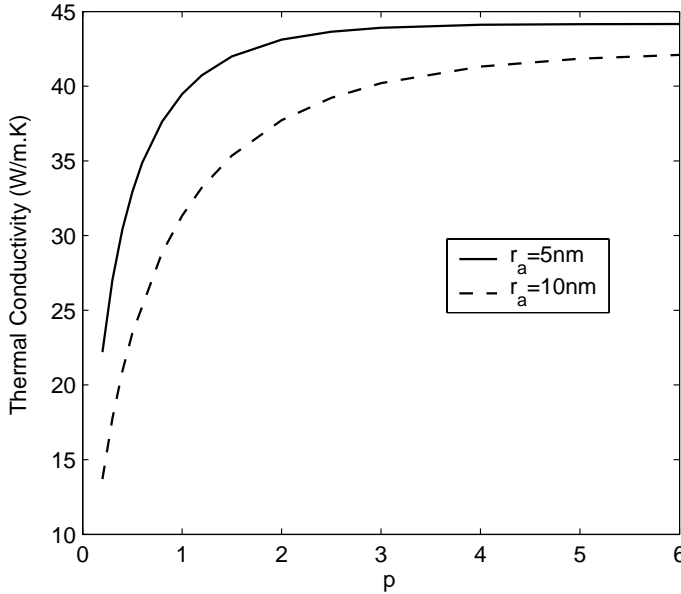


Fig. 5. Lattice thermal conductivity of hollow silicon nanowires as a function of  $p$  for  $T = 300\text{ K}$ . Others are same as in Fig. 4.

boundary scattering is the dominant phonon scattering mechanism in the hollow nanowire.

To clearly elucidate the effect of the phonon scattering by inner wall on the thermal conductance, we display the influence of the index  $p$  [Eq. (8)] on the thermal conductivity in the hollow nanowire, as shown in Fig. 5. It can be found that the thermal conductivity always monotonically decreases with the decrease of the index  $p$ , and the change at small  $p$  ( $<1.5$ ) faster than at bigger  $p$ . The thermal conductivity approaches a constant value When  $p > 2.5$  and  $p > 3.0$  for  $r_a = 5\text{ nm}$  and  $10\text{ nm}$ , respectively. These results indicate that the influence of  $p$  on the thermal conductivity is obvious and is different for different inner radius. In fact, the appropriate value of the index  $p$  should be adjusted according to the experimental thermal conductivity, which is still not be reported as far as we know. Fortunately, it does not influence the qualitative conclusions made above.

#### 4. Summary

In conclusion, we have presented a numerical calculation of the thermal conductivity in a hollow silicon cylindrical nanowire. We consider the modification of phonon dispersion due to the spatial confinement and all important phonon relaxation mechanisms, such as three-phonon Umklapp scattering, mass-difference scattering, phonon-electron scattering, and boundary scattering. At fixed outer radius, the thermal conductivity always decreases with the increase of the inner radius. The boundary scattering leads to a significant decrease of the lattice

thermal conductivity, and is the dominant scattering process. In spite of the effect of Umklapp scattering, mass-difference scattering, or phonon-electron scattering on the thermal conductivity is dependent on the inner radius, the boundary scattering is more sensitive to the variation of the inner radius. We think that the present work will be helpful to understand the properties of the silicon nanotube. Note that the model is also suitable to deal with similar structures made from other semiconductor material.

## Acknowledgments

This work was supported by the National Natural Science Foundation of China, Chinese Academy of Sciences.

## References

1. N. A. Melosh, A. Boukai, F. Diana *et al.*, *Science* **300**, 112 (2003).
2. Y. N. Xia, P. D. Yang, X. G. Sun *et al.*, *Adv. Mater.* **15**, 353 (2003).
3. C. L. Tien and G. Chen, *ASME Journal of Heat Transfer* **116**, 799 (1994).
4. K. Schwab, E. A. Henriksen, J. M. Worlock and M. L. Roukes, *Nature* **404**, 974 (2000).
5. L. G. C. Rego and G. Kirczenow, *Phys. Rev. Lett.* **81**, 232 (1998).
6. M. P. Blencowe, *Phys. Rev.* **B59**, 4992 (1999).
7. M. C. Cross and R. Lifshitz, *Phys. Rev.* **B64**, 085324 (2001).
8. D. H. Santamore and M. C. Cross, *Phys. Rev. Lett.* **87**, 115502 (2001); *Phys. Rev.* **B63**, 184306 (2001).
9. W.-X. Li, K.-Q. Chen, W. H. Duan *et al.*, *Appl. Phys. Lett.* **85**, 822 (2004); *J. Phys.: Condens. Matter* **16**, 5049 (2004); *J. Phys. D: Appl. Phys.* **36**, 3027 (2003).
10. B. A. Glavin, *Phys. Rev. Lett.* **86**, 4318 (2001).
11. A. Balandin, *Phys. Low-Dim. Struct.* **1/2**, 1 (2000).
12. A. Khitun, A. Balandin and K. L. Wang, *Superlatt. Microstruct.* **26**, 181 (1999).
13. S. G. Volz and G. Chen, *Appl. Phys. Lett.* **75**, 2056 (1999).
14. J. Zou and A. Balandin, *J. Appl. Phys.* **89**, 2932 (2001).
15. X. Lu, W. Z. Shen and J. H. Chu, *J. Appl. Phys.* **91**, 1542 (2002).
16. X. Lu, J. H. Chu and W. Z. Shen, *J. Appl. Phys.* **93**, 1219 (2003).
17. W. Fon, K. C. Schwab, J. M. Worlock and M. L. Roukes, *Phys. Rev.* **B66**, 045302 (2002).
18. S. G. Walkauskas, D. A. Broido, K. Kempa and T. L. Reinecke, *J. Appl. Phys.* **85**, 2579 (1999).
19. D. Y. Li, Y. Y. Wu *et al.*, *Appl. Phys. Lett.* **83**, 2934 (2003).
20. N. Mingo, *Phys. Rev.* **B68**, 113308 (2003).
21. N. Mingo, L. Yang, D. Y. Li and A. Majumdar, *Nano Letters* **3**, 1713 (2003).
22. T. F. Zeng and W. Liu, *J. Appl. Phys.* **93**, 4163 (2003).
23. W. S. Jiang and J. R. Ho, *J. Appl. Phys.* **95**, 958 (2004).
24. S. B. Fagan, R. J. Barierle, R. Mota, A. J. R. da Silva and A. Fazzio, *Phys. Rev.* **B61**, 9994 (2000).
25. G. Seifert, Th. Köhler, H. M. Urbassek, E. Hernández and Th. Frauenheim, *Phys. Rev.* **B63**, 193409 (2001).
26. R. Q. Zhang, S. T. Lee, C.-K. Law, W.-K. Li and B. K. Teo, *Chem. Phys. Lett.* **364**, 251 (2002).

27. J. Bai, X. C. Zeng, H. Tanaka and J. Y. Zeng, *P. Natl. Acad. Sci. USA* **101**, 2664 (2004).
28. Y.-J. Han and P. G. Klemens, *Phys. Rev.* **B48**, 6033 (1993).
29. J. Callaway, *Phys. Rev.* **113**, 1046 (1959).
30. D. C. Gazis, *J. Acoust. Soc. Am.* **31**, 568 (1959).
31. G. A. Slack, *Phys. Rev.* **133**, A253 (1964).
32. P. G. Klemens, in *Solid State Physics*, ed. F. Seitz and D. Turnbull (Academic Press, New York, 1958), Vol 7, p. 1.
33. J. E. Parrott, *Rev. Int. Hautes Tem. Refract.* **16**, 393 (1979).
34. G. P. Srivastava, *The Physics of Phonons* (Adam Hilger, New York, 1990), p. 175.